IEEE Access
Multidisciplinary | Rapid Review | Open Access Journal

Received October 30, 2018, accepted November 19, 2018, date of publication November 27, 2018,
date of current version December 27, 2018.

Digital Object Identifier 10.1109/ACCESS.2018.2883412

A Logarithmic Detection Scheme in BOTDR With Low-Bandwidth Requests

QING BAI[1], XUAN ZHENG[1], DONG WANG[1], YU WANG[1], XIN LIU[1], MINGJIANG ZHANG[1], HONGJUAN ZHANG[1], AND BAOQUAN JIN[1,2]

[1]Key Laboratory of Advanced Transducers and Intelligent Control Systems (Ministry of Education and Shanxi Province), Taiyuan University of Technology, Taiyuan 030024, China
[2]State Key Laboratory of Coal and CBM Co-mining, Jincheng 048000, China

Corresponding author: Baoquan Jin (jinbaoquan@tyut.edu.cn)

This work was supported in part by the National Natural Science Foundation of China under Grant 61805167, in part by the Coal-Bed Methane Joint Research Fund of Shanxi Province, China, under Grant 2015012005 and Grant 2016012011, and in part by the Social Development Project of Shanxi Province Key Research Plan under Grant 201703D321034.

ABSTRACT This paper presents a logarithmic detection scheme for reducing the bandwidth of the data acquisition (DAQ) in a Brillouin optical time domain reflectometer (BOTDR). From the analysis of signal features in frequency-scanning BOTDR, the reduction effect of the proposed detection scheme on the bandwidth of DAQ is investigated theoretically. We implement the scheme and evaluate its influence on the performance of BOTDR over a ∼10-km sensing fiber by employing a digitalizer with bandwidth of only 50 MHz. The experimental results show that the spatial resolution of 1.02 m is achieved even though the bandwidth of DAQ is only 50 MHz. At 100-m end of sensing fiber, the root-mean-square error (RMSE) of Brillouin frequency shift (BFS) is 0.67 MHz corresponding to the strain error of 13.4 $\mu\varepsilon$ and temperature error of 0.66°C. As a comparison, the BFS is likewise acquired by a 200-MHz-bandwidth digitalizer, the RMSE of which is 0.66 MHz corresponding to the strain error of 13.2 $\mu\varepsilon$ and temperature error of 0.65°C, nearly consistent with the former. It is confirmed that the logarithmic detection scheme can be used in BOTDR for reducing bandwidth request of DAQ meanwhile without excessive deterioration of spatial resolution or measurement accuracy.

INDEX TERMS Distributed optical fiber sensor, BOTDR, logarithmic detection, low-bandwidth requests.

I. INTRODUCTION

The Brillouin optical time domain reflectometer (BOTDR) has been widely investigated in recent years because of its capability of measuring the temperature and strain distribution in the fiber [1]–[3]. Its measurement is implemented by figuring out the distribution of Brillouin gain spectrums (BGSs) along the optical fiber. The BGS in single-mode fiber (SMF) has been observed as a Lorenz spectral profile with the Brillouin frequency shift (BFS) of ∼11 GHz at the wavelength of 1550 nm [4]. If the BGSs are detected directly by the data acquisition (DAQ) device, the bandwidth and sampling rate have to be respectively more than 11 GHz and 22 GSa/s according to the Nyquist sampling theorem. This costly and complicated DAQ request definitely increases the data amount, processing time and system cost, which severely discourages the widespread use of Brillouin sensing systems. To avoid having to use such wide-bandwidth DAQ, two types of schemes are mainly proposed in BOTDR to reduce electronic bandwidth.

One type of scheme is realized by embedding a fixed-frequency shifter into the optical probe branch, optical reference branch, or electrical signal channel to down convert the BGS for direct detection. For instance, a high-speed phase-modulator is originally operated as the frequency shifter in the optical probe branch [5]. In the reference beam, a single-frequency Brillouin fiber laser is used as the local light oscillator for enabling the bandwidth less than 500 MHz [6]. Similarly, a Brillouin–erbium fiber laser is also used to pump the reference light, generating the BGS centered at about 420MHz [7]–[9]. An electro-optic modulator driven by a microwave generator is exploited to generate the frequency-shifted reference lightwave to make the BGS centered at near 440 MHz and sampled with the rate of 2 Gsa/s or 4 Gsa/s [10], [11]. Furthermore, the BGS can be also down-shifted converted at ∼175 MHz in electrical signal channel after the photodetector and captured directly by a 5 GSa/s digitizer [12]. However, the measurement range of BFS change in the above schemes is inevitably limited, because it is

determined both by the frequency difference between the real detected BFS and the fixed-frequency shifter, and by the bandwidth of DAQ convertor.

For measuring large-scale BFS change and meanwhile reducing DAQ requirements, another type of scheme is implemented by utilizing a tunable frequency sweeper instead of a fixed-frequency shifter, which is called the frequency-sweeping BOTDR. Its BFS measurement range mainly depends on the frequency-sweeping range of the frequency sweeper and is not limited by the DAQ bandwidth [13]. Initially, an electronic spectrum analyzer following the photodetector is operated under the zero-span mode to scan frequency and obtain the time-domain power traces [14]–[16]. For easy integration, a tunable electric local oscillator (ELO) is utilized to perform spectrum scanning and mix with the detected BGS signal, then the mixed frequency signal is filtered by a bandpass filter (BPF) [17], [18]. It has been reported that the BGS linewidth is ∼170 MHz when the pulse width of injected probe light is 10 ns [19], [20]. Hence, the bandwidth of DAQ in frequency-sweeping BOTDR should be more than 170 MHz at least for 1-m spatial resolution, and 200MHz is commonly used in actual application.

In this paper, we proposed a logarithmic detection scheme in BOTDR, enabling the bandwidth of DAQ within 50 MHz and meanwhile ensuring one-meter resolution. The signal feature of BOTDR based on coherent heterodyne detection and frequency-sweeping method was analyzed. Then, the reduction effect of the logarithmic detection scheme on the bandwidth of the DAQ was illustrated. Subsequently, the scheme was implemented and applied to the BOTDR. The measurement accuracy and pulse response time of the detection scheme were optimized, and their influence on the performance of BOTDR was evaluated over the ∼10 km sensing fiber with one-meter spatial resolution. Eventually, the performances of BOTDR utilizing the digitalizer with bandwidth of 50 MHz and 200 MHz respectively were compared.

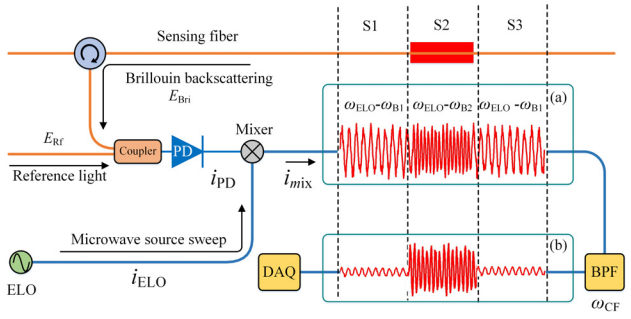

FIGURE 1. Signal flow of BOTDR with coherent heterodyne detection and frequency sweeping method.

II. PRINCIPLE

A. SIGNAL FEATURES OF THE FREQUENCY-SWEEPING BOTDR

The coherent heterodyne detection and frequency sweeping method are commonly used in a BOTDR [21], the signal flow of which is shown in Fig.1. The Brillouin backscattering with BFS information of the detected fiber beats with the reference light in the photodetector (PD). The output signal of photodetector is down-converted by mixing with a tunable ELO. Then the output of the mixer is filtered through a BPF with the center frequency of ω_{CF} and acquired by a data acquisition (DAQ) digitalizer.

The reference light and Brillouin backscattering can be respectively expressed as (1) and (2):

$$E_{Rf}(t) = A_{Rf}\cos(\omega_0 t + \varphi_0) \tag{1}$$

$$E_{Bri}(t) = A_{Bri}\cos[(\omega_0 + \omega_B)t + \varphi_{Bri}] \tag{2}$$

where ω_0 is the frequency of incident light, ω_B is the Brillouin frequency shift, φ_0 and φ_{Bri} are respectively the initial phase of the reference light and the Brillouin backscattering, A_{Rf} and A_{Bri} are respectively the amplitude of the reference light and the Brillouin backscattering.

When these two optical signals pass through the 50:50 coupler, they beat in the photodetector. The photocurrent can be expressed as (3):

$$\begin{aligned} i(t) &= \xi[E_{Rf}(t) + E_{Bri}(t)]^2 \\ &= \xi A_{Rf}^2\cos(2\omega_0 t + 2\varphi_0)/2 \\ &\quad + \xi A_{Bri}^2\cos[2(\omega_0 + \omega_B)t + 2\varphi_{Bri}]/2 \\ &\quad + \xi A_{Rf}A_{Bri}\cos[(2\omega_0 + \omega_B)t + \varphi_0 + \varphi_{Bri}] \\ &\quad - \xi(A_{Rf}^2 + A_{Bri}^2) \\ &\quad + \xi A_{Rf}A_{Bri}\cos(\omega_B t + \varphi_{Bri} - \varphi_0) \end{aligned} \tag{3}$$

where ξ is the responsivity of the photodetector.

Because the frequency respond range of photodetector is 10 kHz∼13.5 GHz, the direct current (DC) part of (3), $\xi(A_{Rf}^2 + A_{Bri}^2)$, is filtered out. The high-frequency component of (3), $\xi A_{Rf}^2\cos(2\omega_0 t + 2\varphi_0)/2$, $\xi A_{Bri}^2\cos[2(\omega_0 + \omega_B)t + 2\varphi_{Bri}]/2$ and $\xi A_{Rf}A_{Bri}\cos[(2\omega_0 + \omega_B)t + \varphi_0 + \varphi_{Bri}]$, can neither be detected for the reason that their frequency all exceed 13.5 GHz. Hence, the actual output current of the photodetector is:

$$i_{PD}(t) = \xi A_{Rf}A_{Bri}\cos[\omega_B t + \varphi] \tag{4}$$

where $\varphi_{=}\varphi_0-\varphi_{Bri}$ is the phase difference between the backscattered light and the reference light.

Considering that the output microwave of ELO is:

$$i_{ELO}(t) = I_{ELO}\cos(\omega_{ELO}t + \varphi_{ELO}) \tag{5}$$

where I_{ELO}, ω_{ELO} and φ_{ELO} are respectively the amplitude, frequency and initial phase of the ELO. Then, the output signal of the mixer can be expressed as (6) :

$$i_{mix}(t) = \xi\eta I_{ELO}A_{Rf}A_{Bri}cos[(\omega_{ELO} - \omega_B)t + \varphi_d)] \tag{6}$$

where η is the conversion loss of the mixer, and $\varphi_d = \varphi_{ELO}$-$\varphi$ is the phase difference. Ignoring the intensity noise and phase difference, the output current of the mixer can be denoted as:

$$i_{mix}(t) = 2\xi\eta\sqrt{2P_{ELO}P_{Rf}P_{Bri}/R_L}cos[(\omega_{ELO} - \omega_B)t] \tag{7}$$

where P_{ELO}, P_{Rf}, P_{Bri} are respectively the power of the ELO, reference light and Brillouin backscattering, R_L is the load resistance.

Supposing that the sensing fiber shown in Fig1 consists of three segments: S1 and S3 with the same BFS denoted as ω_{B1}, and S2 with the different BFS denoted as ω_{B2} larger than ω_{B1}. Regardless of the optical fiber loss, the signal of $i_{mix}(t)$ can be equivalent to a frequency-modulated (FM) sine wave displayed vividly in Fig.1(a). During the frequency-scanning process in BOTDR, the value of ω_{ELO} will be tuned step by step. Only in the case that the measured ω_B equals to the difference of ω_{ELO} and the ω_{CF}, the signal with frequency of ω_{ELO}-ω_B is allowed to pass through the BPF. And the signals with other frequencies will be filtered out. Here, we suppose $\omega_{B2} = \omega_{ELO}$-$\omega_{CF}$, hence the signal (S1 and S3) with frequency of ω_{ELO}-ω_{B1} is filtered out by BPF. The eventually measured signal through BPF is shown in Fig.1(b), equivalent to a sine wave simultaneously modulated by frequency and amplitude.

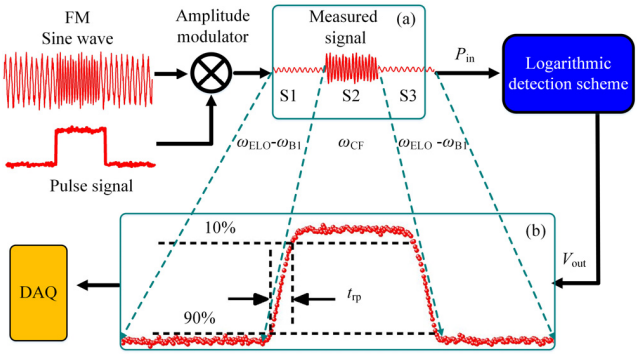

FIGURE 2. Bandwidth-reduced effect of logarithmic detection.

B. BANDWIDTH-REDUCED EFFECT OF LOGARITHMIC DETECTION

Based on the above analysis, the measured signal of the frequency-sweeping BOTDR can be treated essentially as a FM sine wave modulated by a pulse signal, when the frequency of ELO is tuned to ω_{ELO}. It can be simulated as shown in Fig.2(a), which is composed of three segments: S1 and S3 with smaller amplitude and lower frequency of ω_{ELO}-ω_{B1}, S2 with larger amplitude and higher frequency of ω_{CF}. The value of ω_{CF} is generally set to 200MHz in industrial application for one-meter spatial resolution. If the signal is directly connected to DAQ, the bandwidth of DAQ should be more than 200MHz at least so that the signal can be acquired completely [19], [20]. In the paper, a logarithmic detection scheme is utilized before DAQ, and its bandwidth-reduced effect is illustrated in Fig2(b).

The output voltage of logarithmic detection can be given as (8):

$$V_{OUT} = 20 \times k \times \log_{10}(P_{in}/P_{Rf}) \tag{8}$$

where k is the slope voltage coefficient, P_{Rf} is the constant reference power, P_{In} is the power of input signal. The logarithmic detection is capable of converting the input signal to a corresponding output voltage in proportion to the input power in decibel scale. This functionality exactly meets the measurement request of power trace at every scanned frequency point in frequency-sweeping BOTDR.

From (8), it is obvious that the output voltage mainly depends on the input power, which means that the high-frequency signal can be converted to DC voltage signal if the power of the input signal keeps constant. Thus, the measured high-frequency signal in Fig.2(a) can be transformed to a rectangular pulse signal in Fig.2(b) through the proposed logarithmic detection. The high level of the pulse depends on the power of S2, and the low level of the pulse depends on the power of S1 and S3. The rise time of the pulse denoted as t_{rp} hinges on the pulse response time of the logarithmic detection scheme, which is related closely with the spatial resolution of the BOTDR. In order to reach the spatial resolution of one meter, it is necessary to ensure that the value of t_{rp} should be less than 10 ns. According to the relationship between the signal bandwidth and its 10%-90% rise time, the required bandwidth can be given as (9):

$$\text{Bandwidth} \approx \frac{0.35}{t_{rp}} \approx 35\text{MHz} \tag{9}$$

In practical application, the acquiring bandwidth should be nearly 1.5 times of the signal bandwidth. Hence, the bandwidth of 50 MHz can meet the DAQ requests of BOTDR utilizing the proposed logarithmic detection scheme, which is only one quarter of that in a conventional BOTDR with one-meter spatial resolution.

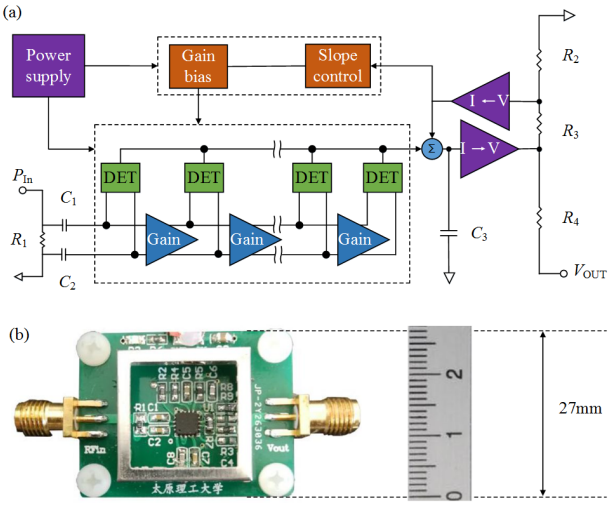

FIGURE 3. Implementation of the logarithmic detection scheme.

III. EXPERIMENTAL RESULTS AND DISCUSSIONS

A. IMPLEMENTATION OF LOGARITHMIC DETECTION SCHEME

The logarithmic detection scheme was implemented as shown in Fig 3. The internal structure of logarithmic detector is shown in Fig.3(a), and the real module is designed in a compact package as shown in Fig.3(b). It mainly consists of several gain stages, each of which is followed by a

square-law detector. This configuration is capable of exactly converting the power of input signal to the output voltage proportionally in decibel scale. The slope voltage coefficient k is controlled by the ratio of R_2 to R_3 and is set to -25mV/dB in the implementation. The gain bias provides the reference power ($P_{\mathrm{Rf}} = 20$ dBm). The capacitance denoted as C_3 is mainly used to filter out the high-frequency ripple of V_{OUT} for improving measurement accuracy. However, the use of C_3 capacitor will inevitably slow down the pulse response time of V_{out}. Hence, the pulse response time should be optimized to meet the requests of spatial resolution by choosing suitable value of C_3 capacitor. Once the value of C_3 is fixed, the measurement accuracy should also be subsequently optimized by picking the appropriate input-signal frequency that determines the main frequency of output voltage ripple.

The impact of C_3 on the pulse response time of V_{out} was investigated by utilizing different capacitance values, including 48.5 pF, 31.5 pF, 21.5 pF, 11.5pF, 6.2 pF and 1.5 pF. The input signal was a sine wave modulated by a rectangle pulse with rise time of 5.68 ns. The power of sine wave was -10 dBm. The measured output voltage with different C_3 values are summarized as shown in Fig.4. It can be seen that the rise time decreases from 270.42 ns to 10.03 ns as the value of C_3 decreases from 48.5 pF to 1.5 pF, as shown in the inset of Fig.4. Thus, the capacitance of C_3 should be 1.5 pF for the rise time of 10.03 ns to ensure the one-meter spatial resolution.

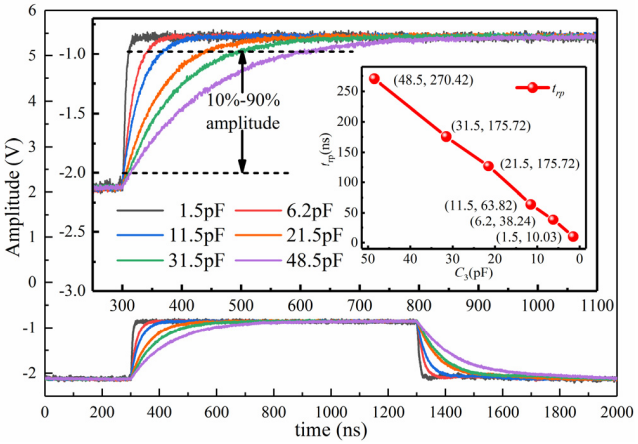

FIGURE 4. Impact of the value of C_3 on the rise time of output voltage.

After the value of C_3 capacitor was fixed at 1.5 pF, the influence of input-signal frequency on the accuracy of V_{out} was evaluated. The input signal was the sine wave as shown in Fig.5(a), and the output signal of the logarithmic detector was a DC voltage trace with ripple as shown in Fig.5(b). We increased the frequency of input signal from 200 MHz to 1 GHz with the step of 100 MHz. The RMSE of output signal at every frequency point was plotted in Fig.5(c). It is found that the RMSE decreases gradually as the input frequency increases, and stays approximately constant since the frequency of input signal exceeds 600 MHz. This variation

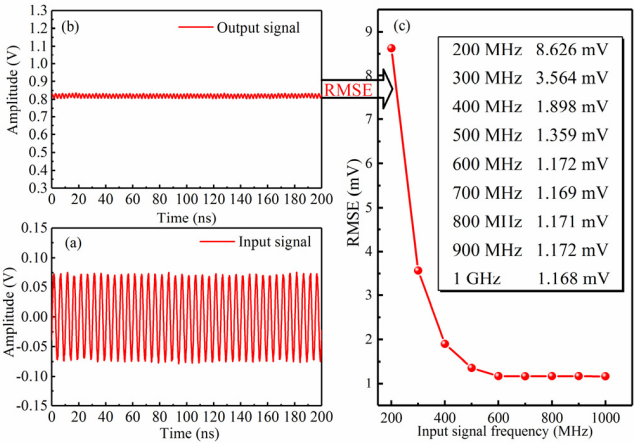

FIGURE 5. Influence of the input signal frequency on accuracy of output voltage.

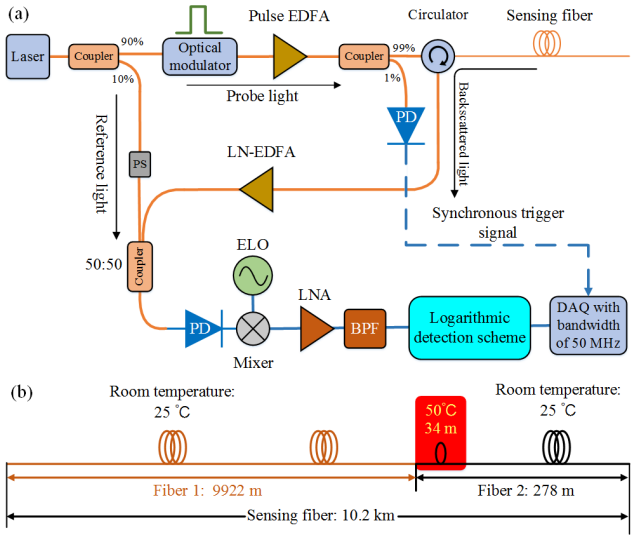

FIGURE 6. Frequency-sweeping BOTDR system with logarithmic detection scheme.

trend arises from the low-pass filter property of the capacitor C_3. When the input frequency increases, the main frequency of output ripple will increase in a logarithmic detector. Instinctively, the RMSE of output ripple is predicted to be almost constant if the frequency of output ripple greatly exceeds the corner frequency determined by the C_3 capacitor. Consequently, the frequency of input signal can be 600 MHz when the C_3 capacitor is 1.5pF, allowing for both shorter pulse response time and higher measurement accuracy.

B. EXPERIMENTAL SETUP OF BOTDR SYSTEM

The experimental BOTDR is schematically shown in Fig.6, which is mainly built based on coherent heterodyne detection and frequency sweeping method. Distinctively, the logarithmic detection scheme is utilized before DAQ, and the bandwidth of the DAQ is only 50 MHz.

As shown in Fig.6(a), the continuous waveform from the laser is divided into probe light and reference light by a 90:10 coupler. The probe light is transformed into optical

pulses with width of 10 ns and repetition rate of 8 kHz by an optical modulator. The pulse light is amplified by a pulse erbium-doped fiber amplifier (Pulse EDFA) and then injected into the sensing fiber with the peak power of 26 dBm. The backscattered light from the sensing fiber is injected into a low-noise EDFA (LN-EDFA). The amplified backscattered light and the reference light scrambled by a polarization scrambler (PS) are beating in a photodetector. The output signal of the photodetector is orderly down-converted by mixing with a tunable ELO, amplified by a low-noise amplifier (LNA), and filtered by a BPF. Then it is connected into the logarithmic detection scheme. A digitalizer with bandwidth of 50 MHz is utilized for acquiring data, which is triggered by an synchronous electrical pulse. The frequencies of ELO were swept with a frequency step of 5 MHz and 2^{13} trace averages.

The configuration of the 10.2 km sensing fiber is shown in Fig. 6(b). The fiber 1 with the length of 9922 m was placed in room temperature of 25°C. The length of fiber 2 was 278 m, 34 m of which was heated to 50°C and the other part of which was located in room temperature.

C. INFLUENCE OF THE LOGARITHMIC DETECTION SCHEME ON THE PERFORMANCE OF BOTDR

As mentioned in III.A section, the pulse response time denoted as t_{rp} and input signal frequency are two key parameters of the proposed logarithmic detection scheme. In this section, we investigated the influence of the two parameters on the performance of BOTDR.

The relationship between t_{rp} and the spatial resolution of BOTDR was explored by multiple BFS measurement utilizing different values of t_{rp}. The t_{rp} was adjusted orderly to 10.03 ns, 12.74 ns, 15.35 ns, 17.94 ns, 19.04 ns, 22.75 ns and 24.68 ns. The measured BFS results corresponding to different t_{rp} is shown in Fig.7.

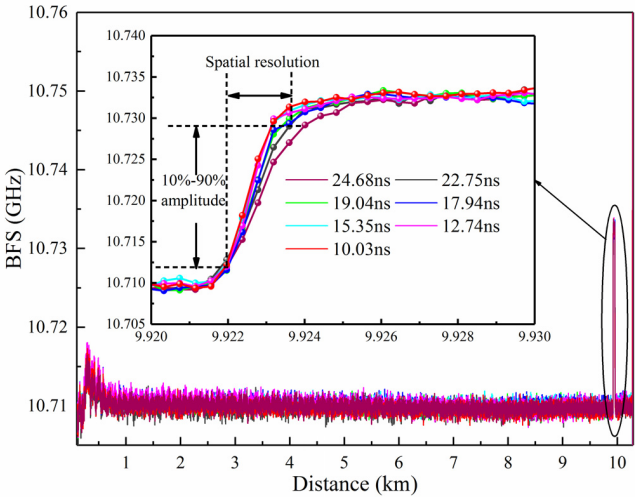

FIGURE 7. BFS distributions versus different t_{rp}.

Taking 10% to 90% of BFS transition edge as the definition of spatial resolution, the spatial resolution versus t_{rp} is plotted as shown in Fig.8. We performed linear fitting on the measured results. It is obvious that the spatial resolution of BOTDR is improved upon the linear scaling as the pulse response time of the logarithmic detection scheme decreases linearly. The adjusted R-square is 0.99882, which indicates the strong linear relationship.

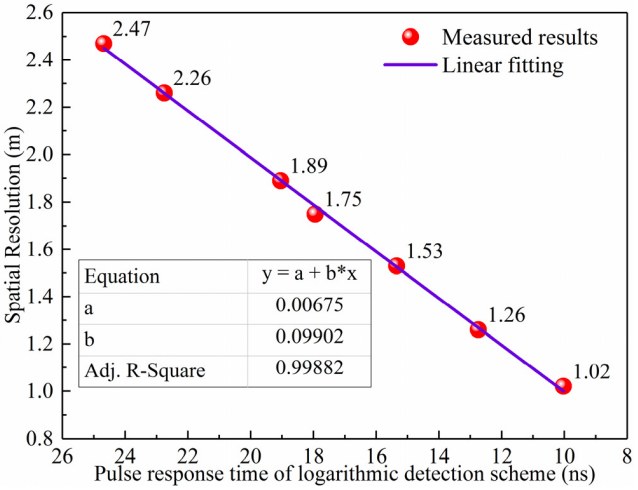

FIGURE 8. Spatial resolution of BOTDR versus t_{rp} of logarithmic detection scheme.

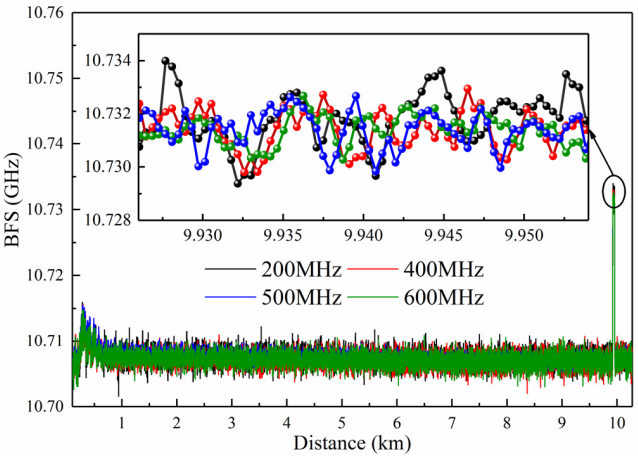

FIGURE 9. BFS distributions versus different center frequency of BPF.

Besides, the influence of input frequency of the logarithmic detection scheme on the accuracy of the BOTDR system was estimated by changing the center frequency of BPF. Four BPFs with different center frequency of 200 MHz, 400 MHz, 500 MHz and 600 MHz were respectively utilized in the experiments. We compared four BFS distribution curves obtained by using the four BPFs, as shown in Fig.9. For further evaluating the measurement accuracy of BOTDR, the measured BFS results of the heated fiber eliminating the rise and fall edge were specially extracted from 9926 m to 9954 m and shown in the inset of Fig.9.

The RMSE and fluctuation amplitude of the measured BFS displayed in the inset of Fig.9 were calculated and figured out in Fig.10. It can be observed that both traces show

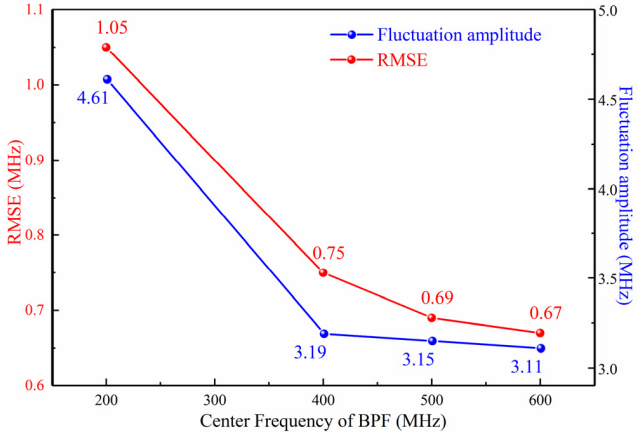

FIGURE 10. RMSE and fluctuation amplitude of the measured BFS versus different center frequency of BPF.

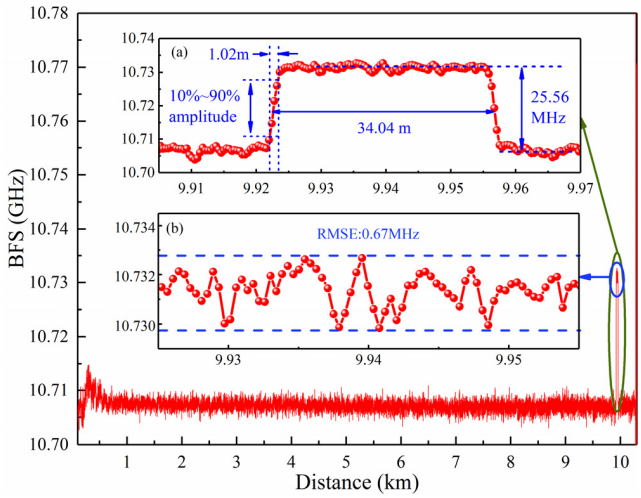

FIGURE 11. Optimal BFS measurement result of BOTDR using the proposed logarithmic detection.

obvious declining trend, which means that the measurement accuracy of BOTDR is improved as the center frequency of BPF increases. We primarily attributed this improvement to the accuracy enhancement of output voltage of the logarithmic detection scheme when the input frequency increases, as shown in Fig.5(c).

From the above analysis, the optimal BFS measurement result can be achieved as shown in Fig.11, when the pulse response time of the logarithmic detection scheme was shortened to 10.03 ns and the input frequency was set at 600 MHz. It can be seen that the BFS starts to increase at 9922 m and the measured length of heated fiber is 34.04m, which is consistent with the sensing fiber shown in Fig. 6(b). The BFS of the heated fiber is 25.56 MHz larger than that at room temperature, consistent with the temperature coefficient of 1.02 MHz/°C. The spatial resolution is 1.02 m. The RMSE of the BFS over the heated fiber is 0.67 MHz corresponding to the temperature accuracy of 0.66°C.

The obtained three-dimensional spectral mapping is shown in Fig. 12. As can be seen clearly, the BFS of the heated

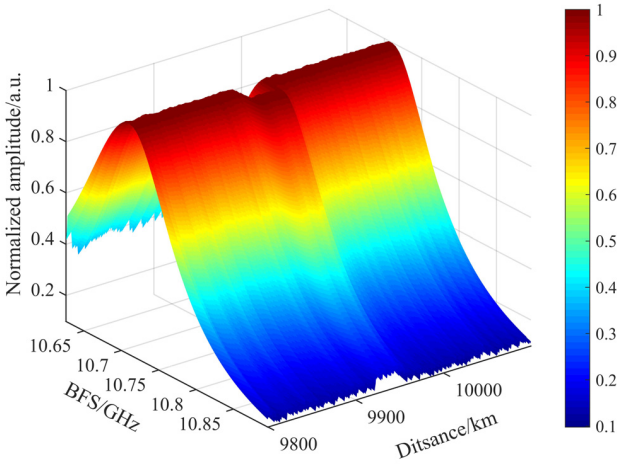

FIGURE 12. Three-dimensional spectral mapping of BGSs.

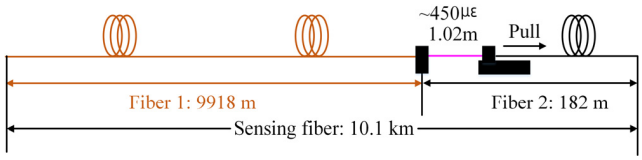

FIGURE 13. Sensing fiber for strain measurement.

fiber is distinctively larger compared with that at room temperature.

D. COMPARISON OF RESULTS OBTAINED BY THE DAQ BANDWIDTH OF 50MHz AND 200MHz

As mentioned in the introduction section, a digitalizer with bandwidth of 200 MHz (more than 170 MHz at least) is required in an actual BOTDR for one-meter spatial resolution. In this paper, the bandwidth of DAQ was reduced within 50 MHz by the proposed logarithmic detection scheme. For comparison, the digitalizers with the bandwidth of 50 MHz and 200 MHz were respectively utilized for measuring BFS. Besides, strain measurement was performed on a 1.02 m fiber to evaluate the spatial resolution more exactly.

The sensing fiber is shown in Fig. 13. The fiber 1 with the length of 9918 m was placed loosely. The length of fiber 2 was 182 m, 1.02 m of which was pulled with the tension strain of 450 $\mu\varepsilon$ and the other part of which kept loosely.

The two measured BFS distributions agree well and are illustrated in Fig.14. The amplitude of BFS peak is 22.43 MHz consistent with the strain coefficient of 0.05 MHz/$\mu\varepsilon$. The measured tension length is 1.02 m according with the length of the pulled fiber in Fig. 13, which means that the spatial resolution of 1.02m was achieved utilizing both electronic bandwidths. The measured BFS at 100-m end of the sensing fiber was utilized to examine the measurement accuracy. The RMSE of BFS respectively obtained by utilizing DAQ bandwidth of 50MHz and 200MHz is 0.67 MHz and 0.66MHz corresponding to the strain accuracy of 13.4$\mu\varepsilon$ and 13.2$\mu\varepsilon$, which indicate little difference.

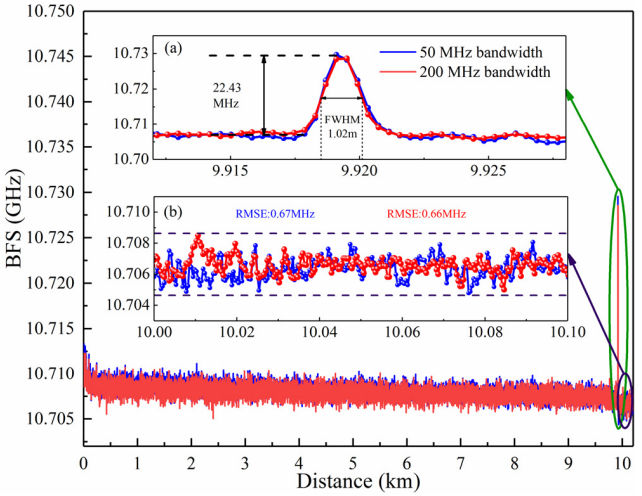

FIGURE 14. BFS comparison between the electronic bandwidth of 50MHz and 200MHz.

Based on the contrast experiment, it is further confirmed that the logarithmic detection scheme can be used in BOTDR without excessive deterioration of spatial resolution or measurement accuracy, even though the bandwidth of DAQ is only 50 MHz.

IV. CONCLUSION

We proposed and experimentally demonstrated a logarithmic detection scheme for reducing the electrical bandwidth requests of a frequency-sweeping BOTDR. The characteristics of microwave signal flow in BOTDR was analyzed, and how the logarithmic detection can decrease the bandwidth request of DAQ was investigated theoretically. Based on the above analysis, we implemented the scheme and tested the performance, including the pulse response time which determines the spatial resolution of BOTDR, and the RMSE of output voltage which affects the measurement accuracy of BOTDR. Eventually, the BFS distribution over the ∼10 km sensing fiber was measured based on the proposed logarithmic detection scheme, utilizing the digitalizer only with the bandwidth of only 50 MHz.

The experimental results indicated that the pulse response time of the logarithmic detection scheme was optimized to reach 10.03 ns to realize the spatial resolution of 1.02 m. The RMSE of measured BFS at the 100m end of 10 km sensing fiber is ∼0.67 MHz, corresponding to the strain error of 13.4 $\mu\varepsilon$ and temperature error of 0.66°C, which is approximately in accordance with that acquired by a digitalizer with the bandwidth of 200 MHz requested in a conventional BOTDR. It is confirmed that the BOTDR with 1-m spatial resolution that only requires 50-MHz DAQ bandwidth is performed using the proposed scheme, for what we believe is the first time. This bandwidth-reduced technique provides a cost-effective solution for DAQ in BOTDR, which greatly decreases the data amount and system cost, and meanwhile consequentially benefits the wide use of BOTDR in industrial applications economically.

REFERENCES

[1] Y. Lu, Z. Qin, P. Lu, D. Zhou, L. Chen, and X. Bao, "Distributed strain and temperature measurement by Brillouin beat spectrum," *IEEE Photon. Technol. Lett.*, vol. 25, no. 11, pp. 1050–1053, Jun. 1, 2013.
[2] X. Bao and L. Chen, "Recent progress in Brillouin scattering based fiber sensors," *Sensors*, vol. 11, no. 4, pp. 4152–4187, 2011.
[3] A. Motil, A. Bergman, and M. Tur, "State of the art of Brillouin fiber-optic distributed sensing," *Opt. Laser Technol.*, vol. 78, pp. 81–103, Apr. 2016.
[4] Z. Yu *et al.*, "Distributed optical fiber sensing with Brillouin optical time domain reflectometry based on differential pulse pair," *Opt. Laser Technol.*, vol. 105, pp. 89–93, Sep. 2018.
[5] H. Izumita, T. Sato, M. Tateda, and Y. Koyamada, "Brillouin OTDR employing optical frequency shifter using side-band generation technique with high-speed LN phase-modulator," *IEEE Photon. Technol. Lett.*, vol. 8, no. 12, pp. 1674–1676, Dec. 1996.
[6] J. Geng, S. Staines, M. Blake, and S. Jiang, "Distributed fiber temperature and strain sensor using coherent radio-frequency detection of spontaneous Brillouin scattering," *Appl. Opt.*, vol. 46, no. 23, pp. 5928–5932, Aug. 2007.
[7] Y. Hao, Q. Ye, Z. Pan, H. Cai, and R. Qu, "Analysis of spontaneous Brillouin scattering spectrum for different modulated pulse shape," *Optik*, vol. 124, no. 16, pp. 2417–2420, Aug. 2013.
[8] Y. Hao, Q. Ye, Z. Pan, H. Cai, R. Qu, and Z. Yang, "Effects of modulated pulse format on spontaneous Brillouin scattering spectrum and BOTDR sensing system," *Opt. Laser Technol.*, vol. 46, pp. 37–41, Mar. 2013.
[9] Y. Hao *et al.*, "Design of wide-band frequency shift technology by using compact Brillouin fiber laser for Brillouin optical time domain reflectometry sensing system," *IEEE Photon. J.*, vol. 4, no. 5, pp. 1686–1692, Oct. 2012.
[10] F. Wang, C. Zhu, C. Cao, and X. Zhang, "Enhancing the performance of BOTDR based on the combination of FFT technique and complementary coding," *Opt. Express*, vol. 25, no. 4, pp. 3504–3513, Feb. 2017.
[11] F. Wang, X. Zhang, Y. Lu, R. Dou, and X. Bao, "Spatial resolution analysis for discrete Fourier transform-based Brillouin optical time domain reflectometry," *Meas. Sci. Technol.*, vol. 20, no. 2, p. 025202, Dec. 2008.
[12] Y. Yu, L. Luo, B. Li, K. Soga, and J. Yan, "Quadratic time-frequency transforms-based Brillouin optical time-domain reflectometry," *IEEE Sensors J.*, vol. 17, no. 20, pp. 6622–6626, Oct. 2017.
[13] S. M. Maughan, H. H. Kee, and T. P. Newson, "57-km single-ended spontaneous Brillouin-based distributed fiber temperature sensor using microwave coherent detection," *Opt. Lett.*, vol. 26, no. 6, pp. 331–333, Mar. 2001.
[14] Y. Lu, Y. Yao, X. Zhao, F. Wang, and X. Zhang, "Influence of non-perfect extinction ratio of electro-optic modulator on signal-to-noise ratio of BOTDR," *Opt. Commun.*, vol. 297, pp. 48–54, Jun. 2013.
[15] Y. Mizuno, N. Hayashi, and K. Nakamura, "Fiber-optic interferometry using narrowband light source and electrical spectrum analyzer: Influence on Brillouin measurement," *J. Lightw. Technol.*, vol. 32, no. 24, pp. 4734–4740, Dec. 15, 2014.
[16] N. Lalam, W. P. Ng, X. Dai, Q. Wu, and Y. Q. Fu, "Performance analysis of Brillouin optical time domain reflectometry (BOTDR) employing wavelength diversity and passive depolarizer techniques," *Meas. Sci. Technol.*, vol. 29, no. 2, p. 025101, Jan. 2018.
[17] H. Ohno *et al.*, "Development of highly stable BOTDR strain sensor employing microwave heterodyne detection and tunable electric oscillator," *Proc. SPIE*, vol. 4596, pp. 74–85, Oct. 2001.
[18] Y. Zhang, X. Wu, Z. Ying, and X. Zhang, "Performance improvement for long-range BOTDR sensing system based on high extinction ratio modulator," *Electron Lett.*, vol. 50, no. 14, pp. 1014–1016, Jul. 2014.
[19] H. Naruse and M. Tateda, "Trade-off between the spatial and the frequency resolutions in measuring the power spectrum of the Brillouin backscattered light in an optical fiber," *Appl. Opt.*, vol. 38, no. 31, pp. 6516–6521, Nov. 1999.
[20] V. Lecoeuche, D. J. Webb, C. N. Pannell, and D. A. Jackson, "Transient response in high-resolution Brillouin-based distributed sensing using probe pulses shorter than the acoustic relaxation time," *Opt. Lett.*, vol. 25, no. 3, pp. 156–158, Feb. 2000.
[21] K. Shimizu, T. Horiguchi, Y. Koyamada, and T. Kurashima, "Coherent self-heterodyne Brillouin OTDR for measurement of Brillouin frequency shift distribution in optical fibers," *J. Lightw. Technol.*, vol. 12, no. 5, pp. 730–736, May 1994.

QING BAI is currently pursuing the Ph.D. degree with the Taiyuan University of Technology. His research interests are distributed optical fiber sensors and engineering applications.

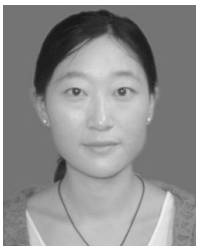

XIN LIU is a Reading Doctor at the Taiyuan University of Technology. Her current research is focused on distributed optical fiber sensors.

XUAN ZHENG is currently pursuing the master's degree with the Taiyuan University of Technology. His research interests are distributed optical fiber sensors.

MINGJIANG ZHANG received the Ph.D. degree in optics engineering from Tianjin University in 2011. He is currently a Professor at the Key Laboratory of Advanced Transducers and Intelligent Control System, Taiyuan University of Technology. His current research interests include optical fiber sensor, semiconductor laser physics, nonlinear laser dynamics, and microwave photonics.

DONG WANG received the Ph.D. degree in instrument science and technology from the Harbin Institute of Technology in 2013. He is currently an Associate Professor at the Key Laboratory of Advanced Transducers and Intelligent Control System, Taiyuan University of Technology. His research interests are in the area of sensors, optoelectronic precision measurement, and optical engineering application.

HONGJUAN ZHANG received the Ph.D. degree in mechatronic engineering from the Taiyuan University of Technology in 2011. She is currently a Professor at the Key Laboratory of Advanced Transducers and Intelligent Control System, Taiyuan University of Technology. Her research interests are in the areas of sensors, optical fiber sensing, and electrical energy saving control.

YU WANG received the M.Sc. degree in electronic engineering from the University of Paris-Sud (Paris XI), France, in 2011, and the Ph.D. degree in electrical and electronic engineering from the University of Cergy-Pontoise, France, in 2014. He is an Associate Professor at the Key Laboratory of Advanced Transducers and Intelligent Control System, Taiyuan University of Technology. His current research interests include vibration detection and optical fiber sensors.

BAOQUAN JIN received the Ph.D. degree in mechatronic engineering from the Taiyuan University of Technology in 2010. He is a Professor at the Key Laboratory of Advanced Transducers and Intelligent Control System, Taiyuan University of Technology, and at the State Key Laboratory of Coal and CBM Co-Mining. His research interests are in the areas of sensors, optical fiber sensing, and engineering application.